Available online at www.sciencedirect.com

ScienceDirect

Physics Procedia 12 (2011) 378–386

Physics Procedia

LiM 2011

Evaluation of Nonlinear Absorptivity and Absorption Region in Fusion Welding of Glass using Ultrashort Laser Pulses

Isamu Miyamoto[a,b]*, Kristian Cvecek[c], Michael Schmidt[b,d,e]

[a] *Osaka University, 1-12, Yama-Oka, Suita, Osaka 565-0871, Japan*
[b] *Erlangen Graduate School of Advanced Optical Technolies (SAOT), Paul-Gordon Str. 6, 91052 Erlangen, German*
[c] *Bayerisches Laserzentrum, Konrad-Zuse Str. 2-6, 91052 Erlangen, Germany*
[d] *Chair of Photonic Technologies, University Erlangen-Nuremberg, Paul-Gordon Str. 6, 91052 Erlangen, Germany*

Abstract

Thermal conduction model is presented, by which nonlinear absorptivity of ultrashort laser pulses in internal modification of bulk glass is simulated. The simulated nonlinear absorptivity agrees with experimental values with maximum uncertainty of ±3% in a wide range of laser parameters at 10*ps* pulse duration in borosilicate glass. The nonlinear absorptivity increases with increasing energy and repetition rate of the laser pulse, reaching as high as 90%. The increase in the average absorbed laser power is accompanied by the extension of the laser-absorption region toward the laser source, suggesting the seed electrons for avalanche ionization are provided mainly by thermal excitation at locations apart from the focus.

Keywords: Nonlinear absorptivity; heat accumulation; thermal conduction; isothermal line; glass; ultrashort laser pulse

1. Introduction

Internal modification of transparent material by ultrashort laser pulses has been drawing much attention due to attractive applications such as formation of optical waveguide [1] and splitter [2], and fusion welding [3,4]. In the internal modification process, the laser energy is absorbed by nonlinear process with multiphoton ionization followed by avalanche ionization [5], and the absorbed laser energy in the free electrons is transferred to the lattice to provide the temperature field in bulk glass. Despite the internal modification process is produced by the nonlinear absorption, study on the nonlinear absorptivity is quite limited.

Schaffer *et al*. reported the dimensions of the internal modification at high pulse repetition rates can be much larger than those of single pulse due to heat accumulation effect [6]. Since then the internal modification with heat accumulation has attracted interest due to its new possibility in internal modification process [7,8], and several authors reported thermal conduction models for internal modification in bulk glass at high pulse repetition rates [9,10]. In their modes, however, the nonlinear absorptivity was simply assumed, and the distribution of the absorbed laser energy was assumed to be of spherical symmetry despite the modified structure extends asymmetrically along

* Corresponding author. Tel.: +81 (0)798-47-1095; Fax: +81 (0)798-47-1095.
E-mail address: miyamoto-i@ares.eonet.ne.jp.

doi:10.1016/j.phpro.2011.03.147

the optical axis [4,8-10]. The laser energy absorbed in the laser-induced plasma has been also simulated based on the rate equation for free electrons at single pulse irradiation in distilled water [11-13]. The model, however, cannot be applied to multi-pulse irradiation at high repetition rates.

Recently, an experimental procedure to measure the nonlinear absorptivity of ultrashort laser pulses in bulk glass was developed [4], assuming the reflection and the scattering of the laser energy by the laser-induced plasma are negligible based on the measurement by Nahen *et al.* [14], and the nonlinear absorptivity was shown to increase significantly with increasing pulse repetition rate at durations of 10*ps* [4] and 400*fs* [15]. It was also reported that the region of the laser energy absorption extends toward the laser source at high pulse repetition rates [4,15], suggesting the absorbed laser energy distributes asymmetrically along the laser axis. The evaluation of the nonlinear absorptivity, however, still remains challenging, since the accuracy of the evaluated nonlinear absorptivity has not been shown, and no thermal conduction model to analyze asymmetrical distribution is available.

In the present paper, a thermal conduction model is presented to simulate the nonlinear absorptivity of ultrashort laser pulses in bulk glass at different energies and the repetition rates of the laser pulse. The accuracy of the simulation is evaluated by comparing with the experimental values. The model shows the increase in the laser absorption needs the extension of the laser absorption region along the laser axis.

2. Experimental evaluation of nonlinear absorptivity

2.1. Cross-section of modified region

Ultrashort pulse laser system from Lumera Laser (Super Rapid; λ=1064*nm*, M^2=1.1) with a pulse duration of 10*ps* was used for internal modification of borosilicate glass sample (Schott D263) with a thickness of 1.1*mm*. The laser beam was focused into the bulk glass by an objective lens for microscope with a numerical aperture (NA) 0.55 at a depth of 260μm from the sample surface. The glass sample was translated transversely to the laser beam at a constant speed of 20*mm/s*. Amongst many parameters influencing the nonlinear absorptivity, we focus here on the energy Q_0 and the repetition rate f of the laser pulse to find out their effects on the dimensions of modified region and thereby the nonlinear absorptivity. Pulse repetition rate was changed between 50*kHz* and 1*MHz*.

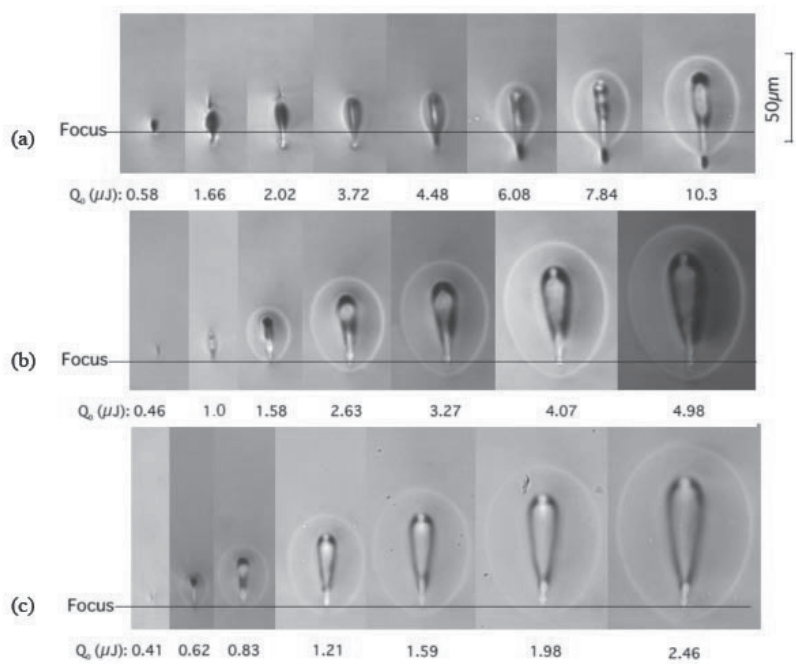

Figure 1. Cross-sections obtained at different pulse energies Q_0 at pulse repetition rates f of (a) 50kHz, (b) 200kHz and (c) 500kHz at 20mm/s in D263. Geometrical focus is assumed to be at the bottom edge of internal modification at threshold pulse energy shown by a horizontal line. (NA0.55, τ=10ps)

Figure 1 shows the cross-sections obtained only at different energies and repetition rates of the laser pulse. Internal modification was realized without cracks except at very limited conditions of low pulse energies at 50*kHz* and 100*kHz*. The modified region consists of a teardrop-shaped inner structure and an elliptical outer structure. The contour of the outer structure was very clearly observed, although it became less clear at average laser power below 300*mW*. The contour of the inner structure was not as clear as that of the outer structure where the modified region changed its tone continuously from the inner structure to the outer structure.

We assumed that the geometrical focus is located at the bottom edge of the inner structure at pulse energy near the threshold of the internal modification, which was approximately 0.4μJ independently of the pulse repetition rate. The bottom edge of the internal structure did not change its vertical position at pulse repetition rate $f \geq 300kHz$ as shown by a horizontal line in Figure 1. At pulse repetition rates $f \leq 200kHz$, however, the bottom edge of the inner structure extended below the geometrical focus at higher pulse energies; at f=50*kHz* the inner structure penetrated through the contour of the outer structure.

2.2. Characteristic temperature of the modified structure

In the present study, the temperature distribution in bulk glass is simulated to determine the isothermal line by the thermal conduction model, and the nonlinear absorptivity is evaluated by fitting the simulated isothermal line to the contour of the experimental modification structures. Then it is essential to evaluate the characteristic temperature of the modified structure. Although the characteristic temperature of the outer structure T_m in borosilicate glass has been speculated in two papers, large difference is found in these values despite the both materials have similar thermal properties; T_m=1,225˚C in Schott AF45 [9] and T_m=560˚C in Schott B270 [10].

We focused laser beam at the interface of overlapped glass plates of D263 moving transversely to the laser beam, and observed the cross-section of the sample by an optical microscope. As shown in Figure 2, the original interface of the glass plates disappears within the outer structure, indicating two glass plates are actually melted and coalesced within the outer region. This is in accordance with the observation of overlap welding in borosilicate glass plates of Corning 0211 by Bovatsek *et al.* [16]. Assuming the glass coalesces at the forming temperature with the viscosity of $10^4 dPas$ [17], the characteristic temperature of the outer structure of D263 is evaluated to be 1,051˚*C*. The forming temperature of AF45 1,225˚*C* [18] agrees with the characteristic temperature speculated in Ref.[9]. On the other hand, the forming temperature of B270 is 1,033˚*C* [19], and the characteristic temperature 560˚*C* in B270 speculated from the relaxation time of the stress based on viscoelastic model is obviously underestimated.

In D263, we refer 1,051˚*C* as “melting temperature” and the outer region as “molten region” hereafter.

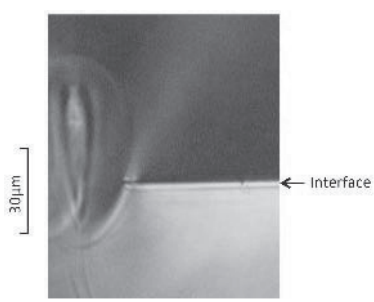

Figure 2. Focused laser beam was irradiated at the interface of two glass plates of D263 (thickness: 1mm, v=20mm/s. The glass plates are welded together within the outer structure of the modified region.

2.3. Experimental evaluation of nonlinear absorptivity

It is reported that the reflection and the scattering of the laser energy by the laser-induced plasma in distilled water are negligible at pulse duration of 30*ps* and 8*ns* [14]. Assuming that the reflection and the scattering of the laser energy by the laser-induced plasma in bulk glass are also negligible at 10*ps* pulse duration, the nonlinear absorptivity A_{Ex} is given by [4]

$$A_{Ex} = 1 - \frac{Q_t}{Q_0} \frac{1}{(1-R)^2}, \tag{1}$$

where Q_0 is incident laser pulse energy, Q_t transmitted laser pulse energy through the glass sample and R Fresnel reflectivity. The validity of Eq.(1) is examined by comparing with the nonlinear absorptivity simulated in 3.2.

The nonlinear absorptivity in the bulk glass was determined by measuring the transmitted laser energy Q_t using a setup shown in the inset of Figure 3(a). The threshold pulse energy for the nonlinear absorption was approximately $0.4\mu J$ in accordance with the threshold energy observed by microscope. The measured nonlinear absorptivity shown by solid lines increases with increasing pulse energy reaching as high as approximately 90%. The increasing rate is larger at higher repetition rates, indicating the nonlinear absorptivity increases with increasing pulse repetition rate.

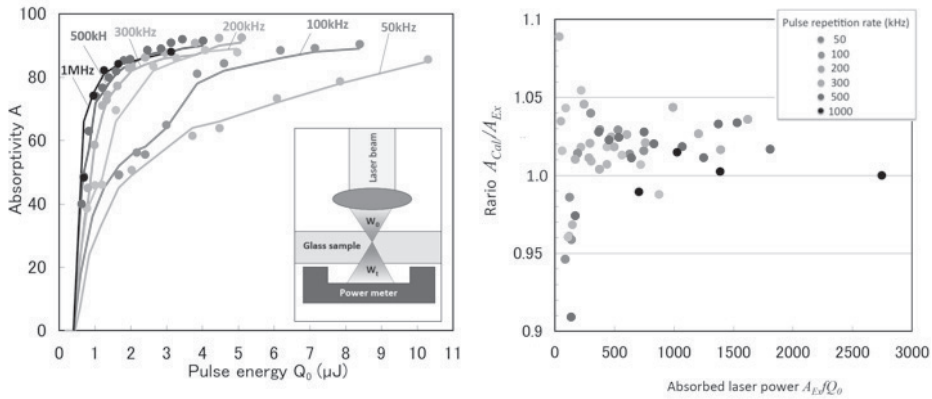

(a) (b)

Figure 3. (a) Nonlinear absorptivity vs. pulse energy at different pulse repetition rates. Solid lines show experimental values, and closed circles simulated values. (b) Ratio of A_{Cal}/A_{Ex} plotted vs. average absorbed lase power W_{ab} ($=A_{Cal}fQ_0$).

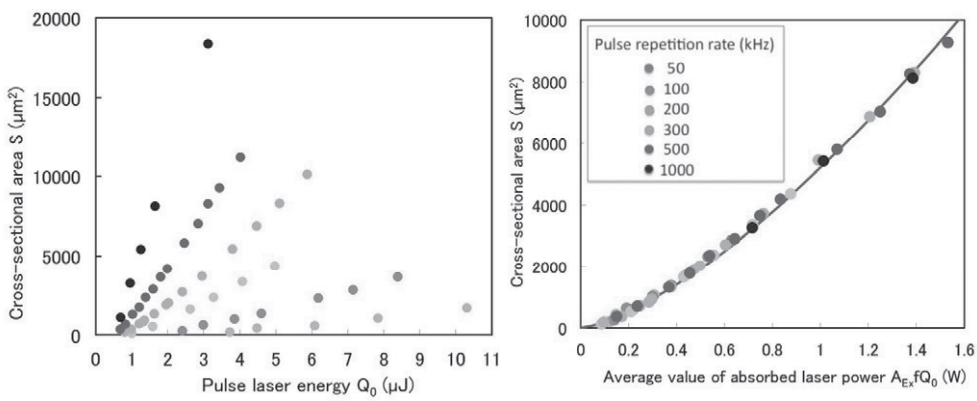

(a) (b)

Figure 4. (a) Cross□sectional area S within isothermal line of T_m vs. laser pulse energy Q_0 at different pulse repetition rates f. (b) S vs. $A_{Ex}fQ_0$. Closed circles are experimental values and solid line simulated.

Figure 4(a) shows the cross-sectional area S of the molten region corresponding to the outer structure plotted as a function of pulse energy Q_0 at different pulse repetition rates, assuming the modified region is elliptical. The cross-sectional area S increases with increasing pulse energy, and the increasing rate increases as the pulse repetition rate increases. In Figure 4(b), S is re-plotted against the average absorbed laser power W_{ab} ($=A_{Ex}fQ_0$). Interestingly, S falls within a narrow band along a single curve, suggesting S is given as a function of W_{ab}. It will be shown that S can be simulated based on the thermal conduction model in 3.2.

3. Simulation of nonlinear absorptivity

3.1. Section headings

When a line heat source with continuous heat delivery of $w(z)$ appears at $x=y=0$ in a region of $0<z<l$ in an infinite solid moving at a constant speed of v along x-axis, the temperature at (x,y,z) with an initial temperature T_0 in a steady state is given by [20]

$$T(x,y,z)=\frac{1}{4\pi K}\int_0^l \frac{w(z')}{s}\exp\left\{-\frac{v}{2\alpha}(x+s)\right\}dz'+T_0, \tag{2}$$

where $s^2=x^2+y^2+(z-z')^2$, K is thermal conductivity and α is thermal diffusivity given by $K/c\rho$ (c=specific heat and ρ=density). It is assumed the thermal properties of the material are independent of temperature, for simplicity. Despite the actual laser beam has finite spot size with pulsed energy delivery, the simple line heat source model with constant heat delivery was used to calculate the temperature at the contour of the molten zone, because the temperature rise at locations apart from the heat source is spatially and temporally averaged. The distribution $w(z)$ is determined by fitting the isotherm of the maximum cycle temperature attained at x where $dT/dx=0$ given by

$$\int_0^l \frac{w(z')}{s}\exp\left\{-\frac{v}{2\alpha}(x+s)\right\}\cdot\left\{\frac{x}{r^3}-\frac{v}{2\alpha}\left(\frac{x}{r}-1\right)\right\}dz'=0 \tag{3}$$

to the contour of the experimental modification structure. Then the nonlinear absorptivity A_{Cal} is given by

$$A_{Cal}=\frac{1}{fQ_0}\int_0^l w(z)dz, \tag{4}$$

and l can be also determined. The advantage of our procedure is that the absolute laser energy absorbed in the bulk glass can be simulated even in the irradiation of multiple laser pulses at high repetition rates. In the following sections, the nonlinear absorptivity ACal and the length of the absorbed region l are simulated.

3.2. Nonlinear absorptivity

We examined a variety of functions for $w(z)$, and satisfactory results were obtained when $w(z)$ is a monotonically increasing function. Here we assumed $w(z)$ is a simple function of z given by

$$w(z)=az^m+b, \tag{5}$$

where a, b and m are positive constants. From Eq.(4), A_{Cal} is written in a form

$$A_{Cal}=\frac{l}{fQ_0}\left(\frac{al^m}{m+1}+b\right). \tag{6}$$

In the simulation, the thermal constants, ρ=2.51g/cm^3 and c=0.82 J/gK (mean value of 20~100 ˚C) [17] were used. Since the thermal conductivity of D263 is not available, we adopted K=0.0096W/cmK (room temperature) of Corning 0211 [21], which is an equivalent material to Schott D263.

Figures 5 shows the examples of the isothermal line of T_m=1051˚C simulated at 500kHz for different m using selected values of a and b, assuming T_0=25˚C. The isothermal line fits well to the contour of the experimental molten region, and l=50μm and A_{Cal}=0.819 are obtained with minor effect of m. The simulated nonlinear absorptivity 0.819 agrees well with the experimental value of A_{Ex}=0.81 (see in Figure 3a). On the other hand, the isothermal line of 3,600˚C is sensitively affected by m, and best fitting was found with m=1, showing that the inner and the outer structures are produced by the common thermal origin. Hereafter m=1 is used for evaluating A_{Cal} and l.

At 50*kHz*, on the other hand, larger discrepancy is observed between the simulated isothermal line of 3,600˚*C* and the experimental inner structure as is shown in Figure 6; the experimental inner structure extends further below z=0 presumably due to self focusing and defocusing by electron cloud [22]. Nevertheless satisfactory agreement is found between the simulated isothermal line of T_m=1,051˚C and the experimental melt contour using 'equivalent' distribution of *w(z)* given by Eq.(5) and resultant value A_{Cal}=85.6% is in good agreement with the experimental value of A_{Ex}=85%. The isothermal line of T_m was adopted for evaluating the nonlinear absorptivity hereafter, since the outer structure is more clearly observed and provides more reproducible nonlinear absorptivity.

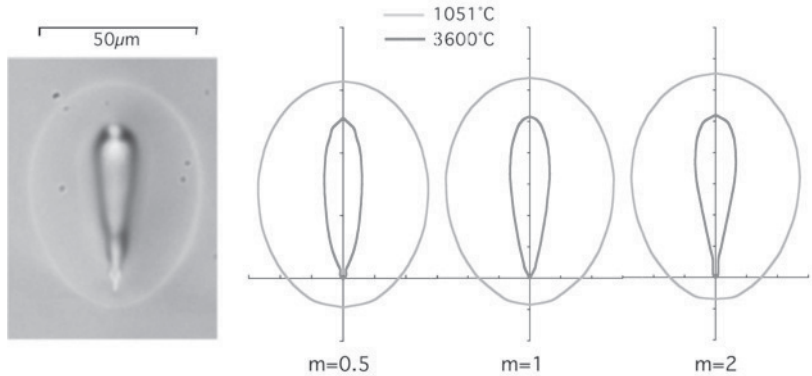

Figure 5. Simulated isothermal lines of 1,051˚C and 3,600˚C at f=500kHz simulated at different values of m (Q_0=1.59μJ, v=20mm/s, T_0=25˚C).

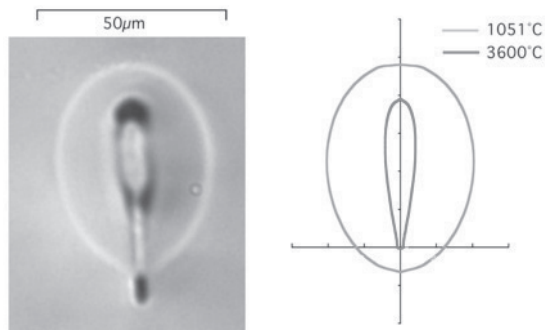

Figure 6. Simulated isothermal lines of 1051˚C and 3600˚C simulated at f=50kHz (Q_0=10.3μJ, v=20mm/s, m=1, T_0=25˚C).

The nonlinear absorptivity A_{Cal} simulated at different values of Q_0 and f is plotted with closed circles in Figure 3(a), showing excellent agreement with A_{Ex}. Excellent agreement is obtained even at 50*kHz* and 100*kHz* in spite of large discrepancy between the isothermal line of 3,600˚C and the inner structure. For analyzing the accuracy of the evaluated values, the ratio of A_{Cal}/A_{Ex} is plotted in Figure 3(b). It is rather surprising that despite the thermal constants at room temperature were used for simulation, A_{Cal}/A_{Ex} ranges in a very narrow region of 1.02 ± 0.03 except for limited condition of W_{ab}<300*mW* where the contour of the molten zone is less clear and deviates significantly from ellipse. Detailed calculation indicated that the bias of 0.02 can be removed to result in $A_{Cal}/A_{Ex}=1 \pm 0.03$ by adopting slightly smaller thermal conductivity of K=0.0093*W/cmK*. The simulated cross-sectional area S is also plotted in Figure 4(b) by a solid line, and is in excellent agreement with the experimental values.

It should be emphasized that A_{Ex} and A_{Cal} are derived independently based on different idea, and that the high accuracy of $A_{Cal}/A_{Ex}=1 \pm 0.03$ is attained under the condition with a wide variety of Q_0 and f. This suggests that both the experimental measurement and the simulation model have the uncertainty less than at least ± 0.03, since the error is accumulated in the calculation of the ratio. This in turn indicates the assumption that the reflection and the scattering of the laser energy by the laser-induced plasma in bulk glass at 10*ps* pulse duration are negligible is

justified. This is considered to be because even though the free electron density exceeds the critical value in bulk glass to become highly reflective, the absorbing plasma with lower electron density existing in the surrounding area can absorb the reflected laser energy [14].

For simulating more precise temperature distribution, one can use complex numerical analysis using temperature dependent thermal properties if they are known. Temperature dependent thermal properties, however, are actually not available, and we believe simple analytical equation using effective value of thermal constants can provide the temperature distribution, which is precise enough to evaluate the nonlinear absorptivity.

3.3. Length of laser absorption region

Neglecting self focusing and defocusing by free electrons, we assumed that the radius of the laser beam propagating in the bulk glass is given by [23]

$$\omega(z) = \omega_0 \sqrt{1 + \left(\frac{M^2 \lambda z}{\pi \omega_0^{\,2} n_g} \right)^2}; \quad \omega_0 = \frac{M^2 \lambda}{\pi NA}, \tag{7}$$

where z is distance from the focus, λ wavelength of the laser beam, M^2 beam quality factor, NA numerical aperture of focusing optics and n_g refractive index of the bulk glass, the laser intensity $I(z)$ at z given by

$$I(z) = \frac{2Q_0}{\pi \tau \omega_0(z)}. \tag{8}$$

Then for given intensity I, z is written in a form of

$$z = \frac{n_g}{NA} \sqrt{\frac{2Q_0}{\pi f \tau I} - \omega_0^{\,2}}, \tag{9}$$

where τ is the pulse duration of the laser beam.

The simulated length of the absorbed region l is plotted *vs.* Q_0 at different pulse repetition rates f with closed circles in Figure 7. It is seen that l increases with increasing Q_0 and the increasing rate ibecomes larger at higher pulse repetition rates. The experimental length l_{Ex} measured from the geometrical focus to the top edge of the inner structure is also plotted in the figure by open circles. An excellent agreement is found between l and l_{Ex}.

In order to find the laser intensity at the top edge of the inner structure, z for given laser intensity I at τ=10ps is plotted for different values of pulse repetition rates in Figure 7. The laser intensity at the top edge of the inner structure is approximately $3.5*10^{11} W/cm^2$ independently of the laser pulse energy Q_0 at f=50kHz where the heat accumulation effect is minimal, suggesting at this intensity or higher the seed electrons for avalanche ionization are provided solely by the mutiphoton ionization.

It is seen that the laser intensity at the top edge of the inner structure $I(l)$ decreases with increasing pulse repetition rate. At Q_0=2μJ, for instance, $I(l)$ decreases with increasing pulse repetition rate, and reaches down to $\approx 10^{10} W/cm^2$ at 1MHz. This value is approximately fifty times as low as that of 50kHz, indicating no seed electrons for avalanche ionization are provided by the multiphoton ionization. Then it is suggested that the seed electrons are provided by thermal excitation at high pulse repetition rates at locations apart from the focus, where high temperature is maintained until the incidence of the next pulse due to the heat accumulation effect. This is supported by the tendency found in Figure 7 that the laser intensity calculated at the top edge of the inner structure decreases with increasing pulse repetition rates. The transient temperature distribution near the laser beam axis, however, cannot be simulated by the line heat source model adopted in this paper. We are now developing a thermal conduction model to simulate the temperature in the laser-irradiated region at the moment of laser pulse incidence with taking into consideration the spatial and temporal distribution of the laser beam propagating in the bulk glass.

The value l in Figure 7 is re-plotted against the experimental average absorbed power W_{ab} in Figure 8. Interestingly again, the data falls on a very narrow band along a single line, indicating W_{ab} is closely related with l. Some scattering of the evaluated values is found at lower value of W_{ab} at 50kHz and 100kHz, because the contour of

the outer structure is not clear enough to evaluate the value l exactly and the molten region deviates significantly from ellipse. The averaged value of the absorbed laser power per unit length W_{ab}/l is also plotted in Figure 8, showing monotonic increase with increasing W_{ab}. This indicates that increase in the absorbed laser energy needs the increase in the length of the absorbed region, when Q_0 or f increases. At high pulse repetition rates it is thus concluded that the increase in the absorption length is caused by thermally excited free electrons due to heat accumulation, that the molten region is increased not only by the heat accumulation [6,9,10] but by the increase in the dimension of the laser-absorption region.

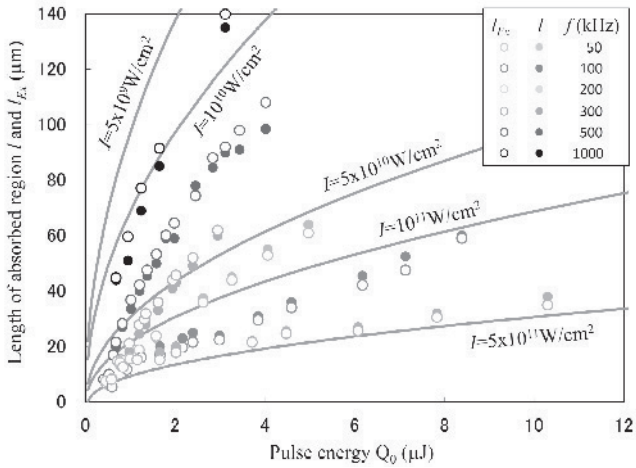

Figure 7. Simulated and experimental length of laser absorbed region vs. pulse energy at different pulse repetition rates. Distance from the focus z at given laser intensity I is plotted by solid lines.

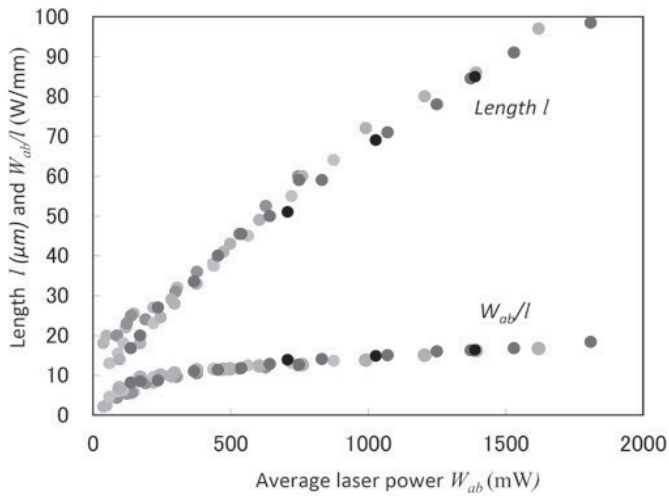

Figure 8. Length of laser absorbed region l and average absorbed laser power per unit length W_{ab}/l vs. averaged absorbed laser power of W_{ab} ($=A_{Cal}fQ_0$) at different energies Q_0 and repetition rates of laser pulse f.

4. Summary

Thermal conduction model with moving line heat source has been developed to simulate the dimensions of the molten region in internal modification of bulk glass by ultrashort laser pulses, and the nonlinear absorptivity and the length of the laser absorption region are evaluated by fitting the isothermal line of melting temperature to the contour of the molten region. The nonlinear absorptivity has been also experimentally determined by measuring the transmitted pulse energy through the glass sample. Excellent agreement is found between experimental and

simulated nonlinear absorptivity with maximum uncertainty of ±3% when pulse energy and pulse repetition rate are widely changed at 10*ps* pulse duration in borosilicate glass of D263. Cross-sectional area of the molten region and the length of the laser-absorption region are closely related with the average absorbed laser power W_{ab}. The nonlinear absorptivity increases with increasing energy and repetition rate of the laser pulse, and the increase in W_{ab} is accompanied by the extension of the laser-absorption region toward the laser source, suggesting the seed electrons for avalanche ionization are provided mainly by thermally excited free electrons at locations apart from the focus at high pulse repetition rates.

Acknowledgements

This work was partially supported by Erlangen Graduate School in Advanced Optical Technologies (SAOT).

References

[1] Davis, K.M.; Miura, K.; Sugimoto, N. N.; Hirao, K.: "Writing waveguides in glass with a femtosecond laser", Opt. Lett., 21 (1996) pp.1729-1731
[2] Homoelle, D.; Wielandy. S.;, Gaeta, A.L.; Borrelli, N.F.: Smith, C.: "Infrared photosensitivity in silica glasses exposed to femtosecond laser pulses," Opt. Lett. 24, (1999) pp.1311-1313
[3] Tamaki, T.; Watanabe, W.; Nishii, J.; Itoh, K.: "Welding of transparent materials using femtosecond laser pulses", Jpn. J. Appl. Phys. 44, (2005) pp. L687-L689
[4] Miyamoto, I.; Horn, A.; Gottmann, J.: "Local melting of glass material and its application to direct fusion welding by *ps*-laser pulses", J. Laser Micro/Nanoengineering, 2, (2007) pp. 7-14
[5] Stuart, B.C.; Feit, M.D.; Herman, S.; Rubenchik, A.M.; Shore, B.W.; Perry, M.D.: "Nanosecond-to-femtosecond laser-induced breakdown in dielectrics", Phys. Rev. B 53, (1996) pp. 1749-1761
[6] Schaffer, C.B.; Garcia, J.F.; Mazur, E.: "Bulk heating of transparent materials using high-repetition-rate femtosecond laser", Appl.. Phys. A 76, (2003) pp. 351-354
[7] Osellame, R.; Chodo, N.; Della, G.; Taccheo, S.; Ramponi, R.; Cerullo, G.; Killi, A.; Morgner, U.; Lederer, M.; Kopf, D.: "Optical properties of wavegyudes written by a 26MHz stretched cavity Ti:Sapphire femtosecond oscillator", Optics Express 13, (2005) pp. 612-620
[8] Nolte, N.; Will, M.; Burghoff, J.; Tuennermann,A.: "Ultrafast laser processing: new options for three-dimensional photonic structures", J. Modern Optics, 51, (2004) pp. 2533-2542
[9] Eaton, S.M.; Zhang, H,; Herman, P.R.; Yoshino, F.; Shah, L.; Bovastek, J.; Ari, A.Y.: "Heat accumulation effects in femtosecond laser-written waveguides with variable repetition rate", Optics Express. 13, (2005) pp. 4708-4716
[10] Sakakura, M.; Shimizu, M.; Shimotsuma, Y.; Miura, K.; Hirao, K.: "Temperature distribution and modification mechanism inside glass with heat accumulation during 250*kHz* irradiation of femtosecond laser pulses", Appl. Phys. Lett., 93 (2008) pp. 231112
[11] Shen, Y.R.: "The principles of nonlinear optics", (New York: Wiley,1984)
[12] Noack, J.; Vogel, A.: "Laser-induced plasma formation in water at nanosecond to femtosecond time scales: Calculation of thresholds, absorption coefficient and energy density", IEEE J. Quant. Elect., 35 (1999) pp. 1156-1167
[13] Arnold, C.L.; Heisterkamp, A.; Ertmer, W.; Lubatschowski, H.: "Computational model for nonlinear plasma formation in high NA micromachining of transparent materials and biological cells", Optics Express,15, (2007) pp. 10303-10317
[14] Nahen, K.; Vogel, A.: "Plasma formation in water by picosecond and nanosecond Nd:YAG laser pulses – Part II: transmission, scattering, and reflection", IEEE J. Quant. El., 2, (1996) pp. 861-871
[15] Miyamoto, I.; Horn, A.; Gottmann, J.; Wortmann, D.; Yoshino, F.: "Fusion welding of glass using femtosecond laser pulses with high-repetition rates", J.Laser Micro/Nanoengineering, 2, (2007) pp. 57- 63
[16] Bovatsek, J. ; Arai, A.; Schaffer, C.B.: "Three-Dimensional Micromachining Inside Transparent Materials Using Femtosecond Laser Pulses: New Applications", Proceedings of CLEO/Europe - EQEC2005 (2005)
[17] http://www.schott.com/special_applications/english/download/d263te.pdf
[18] http://www.schott.com/special_applications/english/download/af45e.pdf
[19] http://psec.uchicago.edu/glass/Schott%20B270%20Properties%20%20Knight%20Optical.pdf
[20] Carslaw, H.S.; Jaeger, J.C.: "Conduction of heat in solids", (Oxford at the Clarendon Press, 1959)
[21] http://www.coresix.com/images/0211.pdf
[22] Tzortzakis, S.; Sudrie, S.M.; Franco, M.; Prade, B.; Mysyrowicz, A.: "Self-guided propagation of ultrashort IR laser pulses in fused silica", Phys. Rev. Lett. 87, 213902 (2001)
[23] Siegman, A.E.; Townsent, S.W.: "Output beam propagation and beam quality from a multimode stable-cavity laser", IEEE J. Quant. Elect., 29 pp.1212-1217 (1993)